Optimized hydrogen generation in a semicontinuous sodium borohydride hydrolysis reactor for a 60 W-scale fuel cell stack

G.M. Arzac [a],[*], A. Fernández [a], A. Justo [a], B. Sarmiento [b], M.A. Jiménez [b], M.M. Jiménez [b]

[a] Instituto de Ciencia de Materiales de Sevilla, CSIC-Univ. Sevilla, Américo Vespucio 49, Isla de la Cartuja, Seville, Spain
[b] Hynergreen Technologies, S.A., Campus Palmas Altas, Seville, Spain

ABSTRACT

Catalyzed hydrolysis of sodium borohydride (SBH) is a promising method for the hydrogen supply of fuel cells. In this study a system for controlled production of hydrogen from aqueous sodium borohydride (SBH) solutions has been designed and built. This simple and low cost system operates under controlled addition of stabilized SBH solutions (fuel solutions) to a supported CoB catalyst. The system works at constant temperature delivering hydrogen at $1\,L\,min^{-1}$ constant rate to match a 60-W polymer electrolyte membrane fuel cell (PEMFC). For optimization of the system, several experimental conditions were changed and their effect was investigated. A simple model based only on thermodynamic considerations was proposed to optimize system parameters at constant temperature and hydrogen evolution rate. It was found that, for a given SBH concentration, the use of the adequate fuel addition rate can maximize the total conversion and therefore the gravimetric storage capacity. The hydrogen storage capacity was as high as 3.5 wt% for 19 wt% SBH solution at 90% fuel conversion and an operation temperature of 60 °C. It has been demonstrated that these optimized values can also be achieved for a wide range of hydrogen generation rates. Studies on the durability of the catalyst showed that a regeneration step is needed to restore the catalytic activity before reusing.

© 2010 Elsevier B.V. All rights reserved.

1. Introduction

Proton-exchange membrane fuel cells (PEMFC) are promising and attractive candidates for meeting the power demands of portable applications [1]. In PEMFCs hydrogen and oxygen are converted by an electrochemical reaction and produce electric energy with water vapour as its sole by-product [2]. For a power generation system based on PEMFC, hydrogen must be supplied at a constant rate and free from carbon monoxide to prevent catalyst poisoning [3]. Among hydrogen storage compounds, sodium borohydride (SBH) has attracted attention due to its high theoretical hydrogen content and the excellent stability of its solution at a high pH value at ambient temperature. Recent review articles on this topic can be found in Refs. [4] and [5]. Furthermore, carbon monoxide free hydrogen can be released from the hydrolysis of SBH alkaline solution in the presence of certain catalysts [6,7]. The maximum storage capacity of sodium borohydride solutions is limited by the formation of hydrated borates during the reaction Eq. (1). In certain conditions these compounds may precipitate from the solution and

damage the catalyst [8].

$$NaBH_4 + (2+X)H_2O = NaBO_2 \cdot XH_2O + 4H_2 + Q \qquad X = 2\text{–}4 \qquad (1)$$
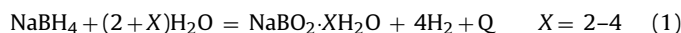
Cobalt boride is a well known and often selected catalyst as it is easy to synthesise and is not as expensive as precious metals [9]. For certain applications, it is preferred to support the catalyst on proper substrates such as Ni foam [10].

Many systems based on SBH hydrolysis have been designed [11–15]. Any design must take into account the exothermic character of the reaction and the fact that constant hydrogen rates only occur at constant temperatures [16]. That control over temperature can be achieved through proper design: immersing a batch reactor in a water bath, operating the reactor under constant flow of reactants and products [11], or just adding stabilized SBH solutions at a certain rate. To the best of our knowledge, there have not been many studies in which control over temperature is achieved by simply controlling the SBH solution supply rate [11–14]. In any case in these papers no simultaneous optimization of storage parameters was found. That is the main reason why we consider of high interest to undertake a research for optimizing both conversion and hydrogen storage capacity in a semicontinuous reactor at constant hydrogen evolution rate. The here presented simple and low-cost design is adapted for portable applications.

These SBH hydrolysis based systems do not store hydrogen in a reversible way but they work at temperatures below 80 °C and

* Corresponding author. Tel.: +34 954489531; fax: +34 954460665.
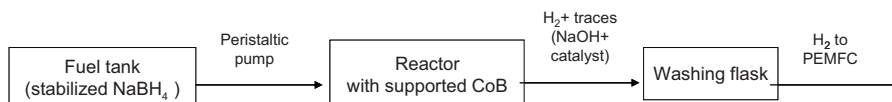E-mail address: gisela@icmse.csic.es (G.M. Arzac).

Fig. 1. Scheme of semicontinuous reactor.

atmospheric pressure. These conditions are simpler and easier to implement than the high temperatures and pressures required for reversible hydrogen storage in light metal hydrides of comparable gravimetric storage capacity [17,18].

In this paper, we present a system to produce hydrogen for a 60 W PEMFC. Hydrogen is intended to be produced at a constant rate of 1 L min^{-1} by maintaining the reaction temperature constant and maximizing conversion and hydrogen storage capacity. Stabilized sodium borohydride solutions were used as fuel and were added at a constant rate to a supported catalyst. Sodium borohydride solutions of different concentrations were supplied to the reactor in different conditions. A first set of experiments was conducted to prove whether it is possible to control the temperature by adding fuel solutions at a certain constant rate. The effect of SBH concentrations, fuel adding velocity and amount of catalyst on the system was also evaluated. In order to improve our first results, a second set of experiments was conducted. We intended to maximize total conversion for each SBH solution concentration, which may imply maximum hydrogen storage capacity. A third set of experiments was carried out to vary the hydrogen generation rate while keeping the optimized parameters found in the second set. Additionally, tests on durability of the catalyst were also performed.

2. Experimental

2.1. Preparation of Ni foam supported catalyst

The supported CoB catalyst was prepared by chemical reduction of CoCl$_2$·6H$_2$O (99% Fluka) aqueous solution with NaBH$_4$ (99% Aldrich) solution stabilized in NaOH (99.3% Sigma), according to Ref. [10]. Nickel foam (Goodfellow 1.6 mm thick, 95% porosity, 20 pores cm^{-1}), was used as the support for the catalyst. Deionised water (MilliQ®) was used to prepare the solutions. Before syntheses Ni foam was cut in 1 cm × 2 cm rectangles and weighted.

Heat treatment conditions were chosen from Ref. [10] searching for a good compromise between maximum activity and adhesion of CoB to the support. Samples were then treated at 573 K (heating rate 1 °C min^{-1}) in pure helium environment for 2 h before cooling to room temperature.

2.2. Characterization of Ni foam supported catalyst

X-ray diffraction measurements were performed using Cu Kα radiation in a Siemens D5000 diffractometer in a Bragg–Brentano configuration in the 2θ angle range of 40–80°.

Scanning electron microscopy (SEM) was performed to study the morphology of samples in a high resolution FEG microscope, Hitachi S5200.

2.3. Hydrogen generation (HG) test

HG tests were performed in a homemade reactor. The reactor was made of stainless steel and had a capacity of 250 ml. Lighter plastic materials could be also used to fabricate the same design. A scheme of the experimental system is presented in Fig. 1. To give an idea of the device volume, the fuel tank also has a maximum volume of 250 ml and the washing flask 100 ml.

For each experiment, a certain amount of supported CoB catalyst was put at the bottom of the reaction chamber. The reactor was then closed, and the NaBH$_4$ solution stabilized in 4.5 wt% NaOH of the selected concentration (wt%) was added through a peristaltic pump at the selected rate. Before measuring flow rate, the hydrogen evolved was bubbled in pure water in order to wash the gas from rest of the fuel solution and eventual powder catalyst. Hydrogen generation rate (HGR, ml min^{-1}) was then measured as a function of time with a previously calibrated volumetric flowmeter. The fuel supply was maintained for 60 min and was then interrupted. Residual hydrogen flow was measured until the hydrogen generation rate was 100 ml min^{-1}. No stirring was performed for the kinetic experiments, except for the stirring action of the evolved hydrogen. Temperature was measured with a thermocouple at the medium height of the reactor.

The average hydrogen generation rate (HGR, ml min^{-1}) was obtained from the plot of HGR vs time. The total conversion (TC) was calculated as $100 \times V/V_{th}$ where V represents the area under the HGR vs time curve in the interval where the hydrogen flow was constant. V_{th} was calculated as the theoretical volume of hydrogen (at room temperature) to be obtained from the total volume of fuel supplied at each particular concentration of sodium borohydride. Gravimetric hydrogen storage capacity (wt%) was calculated from $100 \times M/(M_{sol} + M_{cat})$ where M represents the total mass of hydrogen generated during the experiment in the constant flow region; M_{sol} represents the total mass of the solution supplied; and M_{cat} represents the total mass of CoB used, including the support.

For the first set of experiments, SBH fuel solution concentrations (between 9 and 28 wt%), fuel feed rate and amount of catalyst were varied.

For the second set of experiments, SBH fuel solution concentration was also varied between 9 and 28 wt%. The fuel feeding rate was chosen for each SBH concentration to supply the exact amount of SBH in the time to produce 1.15–1.2 L min^{-1} hydrogen. This 15–20% excess in HGR was set to ensure, between the fluctuations of the system, that this value is never lower than 1 L min^{-1} in order not to damage the PEMFC. The amount of catalyst was chosen to be in excess in each case.

3. Results and discussion

3.1. Theoretical considerations

An important requirement for real applications is to maximize the gravimetric hydrogen storage capacity (HSC, wt%) of the system. Without taking into account the reactor, HSC can be defined according to Eq. (2). In the term $\Sigma M_{reactants}$ we include the mass of SBH, the mass of H$_2$O and the mass of the eventual catalyst (including support).

$$\text{HSC (wt\%)} = 100 \times \frac{M_{\text{hydrogen generated}}}{\sum M_{\text{reactants}}} \qquad (2)$$

HSC (wt%) can be written as a function of NaBH$_4$ concentration for aqueous mixtures in an idealization without considering the mass of catalyst and considering a 100% yield of the reaction (HSC potential, a summary is represented in Fig. 2). For concentrations lower than 35.5 wt% SBH (solubility point) we speak about solutions that can be used as fuel and for higher concentrations we merely refer to mixtures. Using Eq. (2) and taking into account the stoichiometry
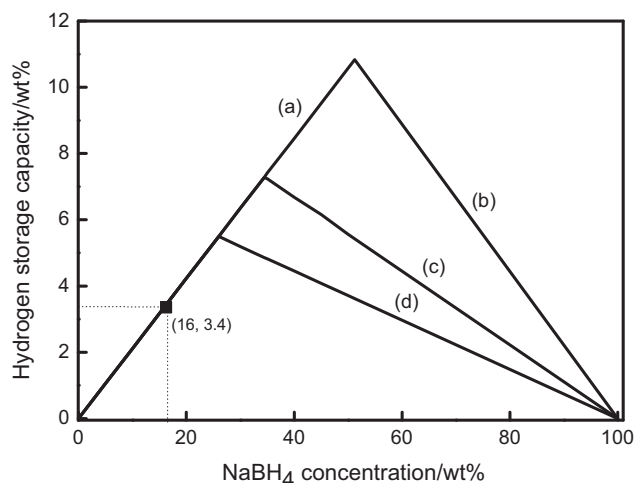
Fig. 2. Theoretical maximum hydrogen storage capacity (gravimetric, wt%) as a function of wt% concentration of $NaBH_4$ in the absence of catalyst. HSC curve in conditions of excess of water (a). HSC curves in conditions of excess of SBH for $X = 0$ (b), $X = 2$ (c) and $X = 4$ (d).

of the reaction (1), HSC (wt%) can be expressed as a function of SBH concentration for different values of the hydration factor X.

In the region of stoichiometrical excess of water ((a) zone from Fig. 2), HSC is only a function of SBH concentration according to Eq. (3).

$$HSC\ potential\ (wt\%) = 8 * \frac{wt\%\ NaBH_4\ in\ solution}{37.83} \quad (3)$$

It is important to emphasize that the validity of (3) is between SBH concentrations equal to 0 and x_0, where x_0 represents the maximum concentration of SBH in stoichiometrical excess of water regime. For higher values of x_0, stoichiometrical excess of SBH must be considered with subsequent economical losses. The x_0 factor varies with the value of the hydration factor X according to Table 1.

In the region of stoichiometrical excess of SBH, HSC is written as set in (4) where W is a stoichiometrical factor that varies with the value of X according to Table 1.

$$HSC\ potential\ (wt\%) = 8 * \frac{(100 - wt\%\ NaBH_4\ in\ solution)}{37.83 * W} \quad (4)$$

From these considerations, many conclusions can be extracted. First of all, in the region of SBH concentrations where this compound is soluble, one can associate a maximum HSC (max. HSC, wt%) for each SBH fuel solution concentration. This is a potential HSC, since 100% yield of the reaction must be reached. The actual HSC for a particular experiment can be either expressed as (2) or as (5). Eq. (5) makes it possible to combine economical aspects, such as total conversion (TC defined in the experimental part), with experimental design aspects such as the fuel solution concentration.

$$HSC\ (wt\%) = \frac{HSC\ potential * TC}{100} \quad (5)$$

Table 1
Values of x_0, (maximum concentration of SBH with stoichiometric excess of water) HSC and W for different hydration factor values of sodium borate (X, see Eq. (1)).

X	x_0[a] (wt%)	HSC[b] (wt%)	W[c] (Eq. (4))
0	51.2	10.8	1.0
2	34.44	7.28	1.9
4	26	5.5	2.85

[a] Maximum concentration of SBH with stoichiometric excess of water.
[b] Corresponding maximum achievable HSC.
[c] Stoichiometrical value in Eq. (4).

In addition, and in agreement to what has been observed by other authors [6], $NaBO_2$ hydration lowers the maximum achievable HSC of the system from 10.8% to even 7.3% when considering $X = 2$ (see zone c in Fig. 2). Further limitations to HSC for $NaBH_4$ solutions are related to $NaBO_2$ solubility (33 g/100 g H_2O or 24.81 wt%) and the fact that precipitation can damage the catalyst described above. At the limit of the $NaBO_2$ solubility point, $NaBH_4$ concentration is approximately 16 wt%, with maximum HSC of 3.38%. This limit could be overcome by operating the reactor at temperatures higher than 60 °C. In this range, sodium borates ($NaBO_2 \cdot 4H_2O$) would melt with apparently no damage to the catalyst and even enhancing the diffusion of reactants [14,17].

3.2. Ni foam supported catalyst

Characterization of the Ni foam supported catalyst has been carried out by XRD and SEM analysis.

Fig. 3(a) shows the Ni foam substrate before and after catalyst deposition. The supported catalyst shows a porous microstructure that favours good accessibility of reactives to the catalysts and an increase in exposed surface.

The XRD pattern in Fig. 3(b) corresponds, as previously reported by other authors [8], to an amorphous or nanocrystalline CoB phase characterized by a very broad and low intensity peak between 40 and 50 2θ degrees. The identified sharp peaks correspond therefore to the Ni foam support. The intensity ratio between peaks is not significant in this case due to the texture of the nickel foam with a major roughness and large pores.

3.3. Kinetic experiments

3.3.1. Dependence of HGR on SBH concentration, fuel addition rate and amount of catalyst

In the first set of experiments (Table 2), kinetic measurements were performed for different SBH wt% concentrations while varying fuel addition rate and the amount of supported catalyst.

As expected, under certain conditions, a fuel delivery with controlled velocity leads to a constant temperature and consequently, a constant hydrogen generation rate.

Comparison of the results from experiments 1.c–e shows that, for a given amount of supported catalyst, there is a certain fuel rate that makes it possible to obtain stable and constant hydrogen generation rate. From experiments 1.d and 1.f, it can be seen that at a fixed fuel addition velocity, hydrogen generation rate increases with the amount of the catalyst. This result enables us to establish, at least qualitatively, that it is possible to tune the final HGR by varying the amount of catalyst at a constant fuel rate.

From experiments 1.a, 1.b, 1.f and 1.g, it seems to be possible to find the conditions to produce hydrogen at the desired constant rate in the interval of 1 ± 0.2 L min^{-1} at constant temperatures. In these experiments, which can be considered to be at an approximately similar fuel addition rate, total conversion decreases with SBH concentration. This result has a negative economical impact since SBH is left unreacted and also has a negative influence on the final HSC. As shown in Fig. 2, the more concentrated the SBH fuel solution, the higher is the potential HSC. However the final HSC is lowered here by the decrease in TC as expressed in (5). We found that the highest HSC is associated to the SBH 14 wt% solution (exp 1.b). These results can be interpreted as follows: for a fixed rate of hydrogen generation (in this section 1 L min^{-1}) there is a minimum amount of SBH to be delivered per minute. In the particular case of experiments 1.a, 1.b, 1.f and 1.g, the higher the SBH concentration the higher the excess over this minimum. This stoichiometrical excess leaves a high amount of reactant unreacted, with the negative consequences described above.
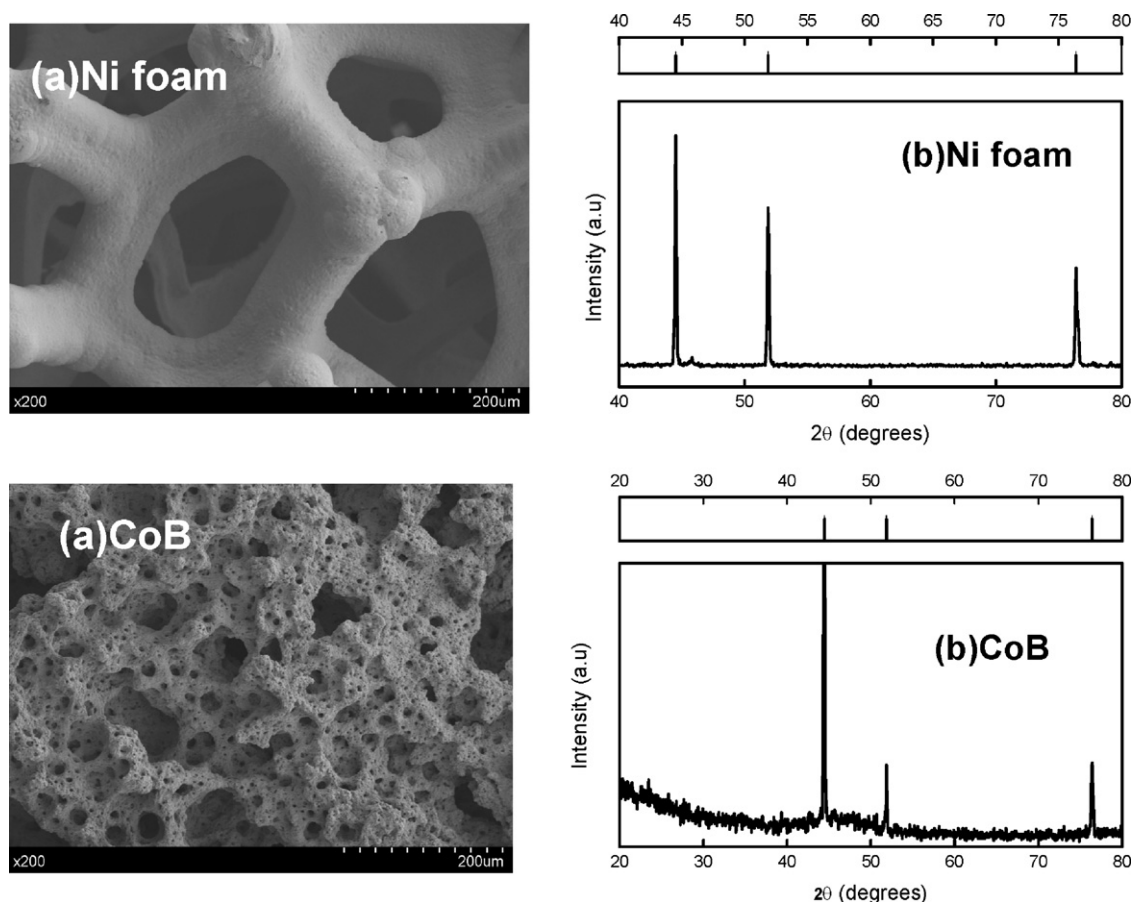
Fig. 3. (a) SEM image of the Ni foam substrate before and after deposition of the CoB catalyst. (b) XRD pattern of the Ni foam substrate without and with supported CoB catalyst. In both XRD, the upper layer corresponds to Ni^0 pattern.

The second set of experiments goes in this direction. In an excess of catalyst, for each SBH concentration, we worked near minimum stoichiometrical SBH addition rate conditions to achieve the desired $1 L min^{-1}$ hydrogen generation. As described in the experimental part, and considering the final application, we supplied the reactor with a 15% excess of the theoretical fuel addition rate for each SBH concentration. This procedure takes into account the fact that excess of hydrogen can be regulated by valves but a defective supply could cause damage to the PEMFC. This type of experiment will be discussed in the following section.

3.3.2. Experiments under variable fuel rate

As described in the previous section, we designed a second set of experiments to improve the TC and HSC values of the first. Table 3 summarizes the results. Fig. 4 shows the evolution of HGR and temperature as a function of time for the most representative experiments (2.a–c and 2.e).

From data in Table 3 and Fig. 4, it can be seen that for experiments 2.a–c constancy in temperature and HGR was achieved. Total conversion was improved to 90–100%. HSC was also improved, since for SBH concentrations 9, 14 and 19 wt% this parameter almost reached its maximum value. The difference between the experimental HSC and the theoretical potential HSC is exclusively due to the fact that conversion was lower than 100%. No significant effect of the amount of catalyst on HSC was found under these optimised experimental conditions.

Optimum conditions were found for 19 wt% SBH fuel solution at $2.5 ml min^{-1}$ addition rate to generate constant $1.16 L min^{-1}$ hydrogen (Table 3, exp 2.c,) with a TC of 90% and a HSC of 3.5 wt%. Temperature was maintained constant around $60\,^\circ C$ what represents a good heat management in this system. These values represent a global optimization of different parameters at the same time. Although values of HSC higher than 6 wt% have been reported [16,19,20] no constant hydrogen rate release was searched or no heat management was pursued. In some cases an external

Table 2
Parameters (as described in the text) for the first set of hydrogen generation kinetic measurements.

Exp.	NaBH$_4$ concentration (wt%)	Mass of supported CoB (mg)	Fuel addition rate (ml min^{-1})	HGR (L min^{-1})	TC (%)	HSC (wt%)	HSC[a] potential (wt%)	T ($^\circ$C)
1.a	9	470	4.4	1.06	96	1.8	2	40
1.b	14	383	3.4	1.20	87	2.5	3	50
1.c	19	52	2.71	≤0.1	–	–	4	–
1.d	19	51	3.4	0.4	25	0.9	4	38
1.e	19	52	7.8	≤0.1	–	–	4	–
1.f	19	107	3.4	1	55	2.1	4	50
1.g	28	90	3.4	0.85	20	1.1	6	45

[a] Considering that we are below the x_0 value for $X = 2$ in all cases.

Table 3
Parameters (as described in the text) for the second set of hydrogen generation kinetic measurements.

Exp.	NaBH$_4$ concentration (wt%)	Mass of supported CoB (mg)	Fuel addition rate (ml min^{-1})	HGR (L min^{-1})	TC (%)	HSC (wt%)	HSC[a] potential (wt%)	T (°C)
2.a	9	458	4	1.13	95	1.9	2	47
2.b	14	560	3	1.20	99	3	3	57
2.c	19	675	2.5	1.16	90	3.5	4	60
2.d	23.5	644	1.5	Variable	–	–	5	Increasing
2.e	28	1019	1.6	Variable	93	5.6	6	Increasing

[a] Considering that we are below the x_0 value for $X = 2$ in all cases.

thermostatic bath was needed [19] and this is avoided with our experimental set-up.

Experiments carried out with SBH fuel solutions of 23.5 and 28 wt% deserve special attention. For these solutions, neither the temperature nor the HGR were kept constant. Temperature increased constantly, HGR fluctuated significantly and finally went out of control when temperature was higher than 60 °C. In addition, when measurements were possible (experiment 2.e), TC and HSC values were lower. These findings can be explained by two reasons. On the one hand, there could be an effect on temperature control: for a fixed amount of SBH in solution, the more concentrated the solution, the lower the amount of water. This lower amount of water may not compensate for the heat liberated by the reactions. On the other hand, NaBO$_2$ precipitation in highly concentrated SBH solutions causes occlusion over the catalyst, impeding accessibility to the catalytically active sites.

Fig. 5(a) shows the SEM images of the supported catalysts after use in experiments 1.a (SBH 9 wt%) and 1.g (SBH 28 wt%) showing the effect of borate deposition when porosity almost disappears for the experiments with higher concentrated SBH solutions. XRD pattern in Fig. 5(b) also shows the absence of borates on the surface of the catalyst (for SBH 9 wt%) and the deposition of NaB(OH)$_4$ for the SBH 28 wt% experiment.

This second set of experiments clearly shows that with the experimental set-up presented here it is possible to maximize TC and HSC for SBH concentrations up to 19 wt%. The optimization of higher concentrations is limited under the experimental conditions presented here.

Finally it is of interest to emphasize that according to data in Fig. 4, the run-in periods, before stabilization of the constant hydrogen flow, are always below 5 min for the optimized conditions (2.a–c). This result is also of interest for the practical use of the device for feeding a fuel cell stack.

3.3.3. Experiments to control the HGR under optimized conditions

A new set of experiments was undertaken to explore a wide range of HGR values above and below the up to now discussed 1 L min^{-1}. In Table 4 data are summarized for experiments carried out under excess of supported catalyst for our stabilized 19 wt% SBH fuel solutions. Fuel addition rate has been calculated and supplied to the reactor to produce 0.25 and 0.6 L min^{-1} HGR. The data show that the optimized parameters found in experiment 2.c (also included in Table 4) can be obtained for an extended HGR range. The experimental curves for experiments 3.a and 3.b are shown in Fig. 6(a). The run in period increases as the HGR decreases which explains the slight decrease in TC as the hydrogen generated in this period is not taken into consideration for the calculation of this parameter.

For the same SBH 19 wt% fuel solution experiments were carried out in the same reactor to achieve HGR values higher than
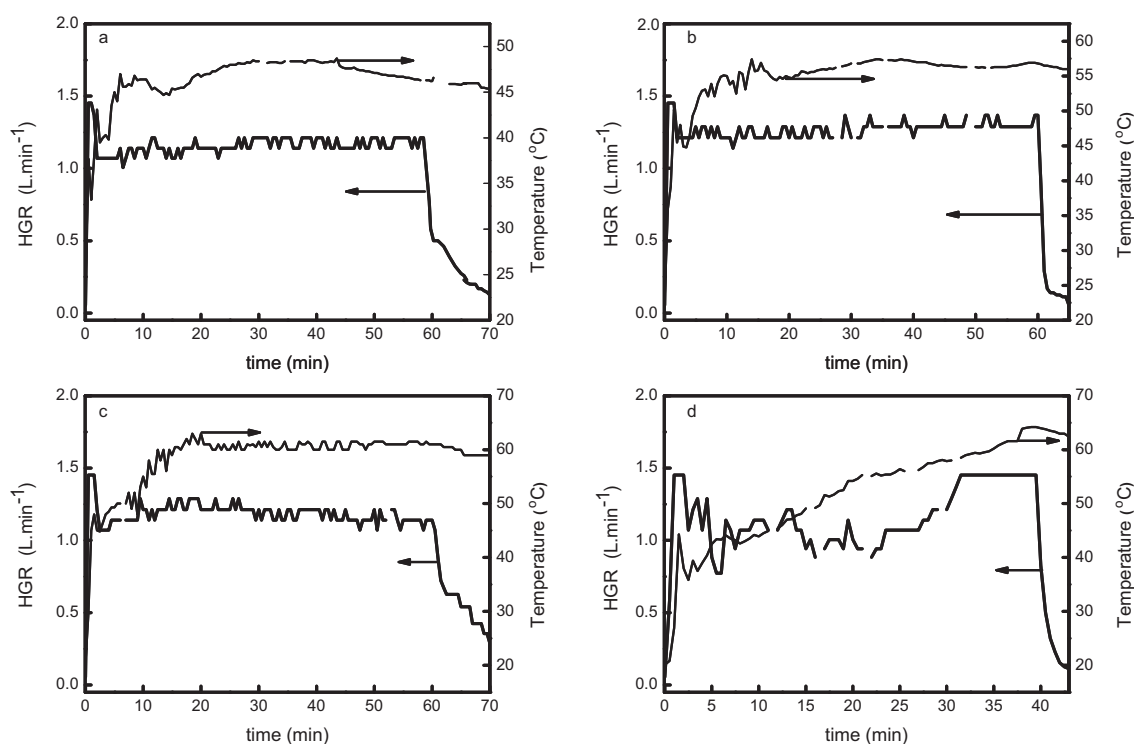

Fig. 4. Evolution of hydrogen generation rate and temperature during representative experiments of the second set. (a) Exp 2.a, (b) exp 2.b, (c) exp 2.c, (d) exp 2.e.
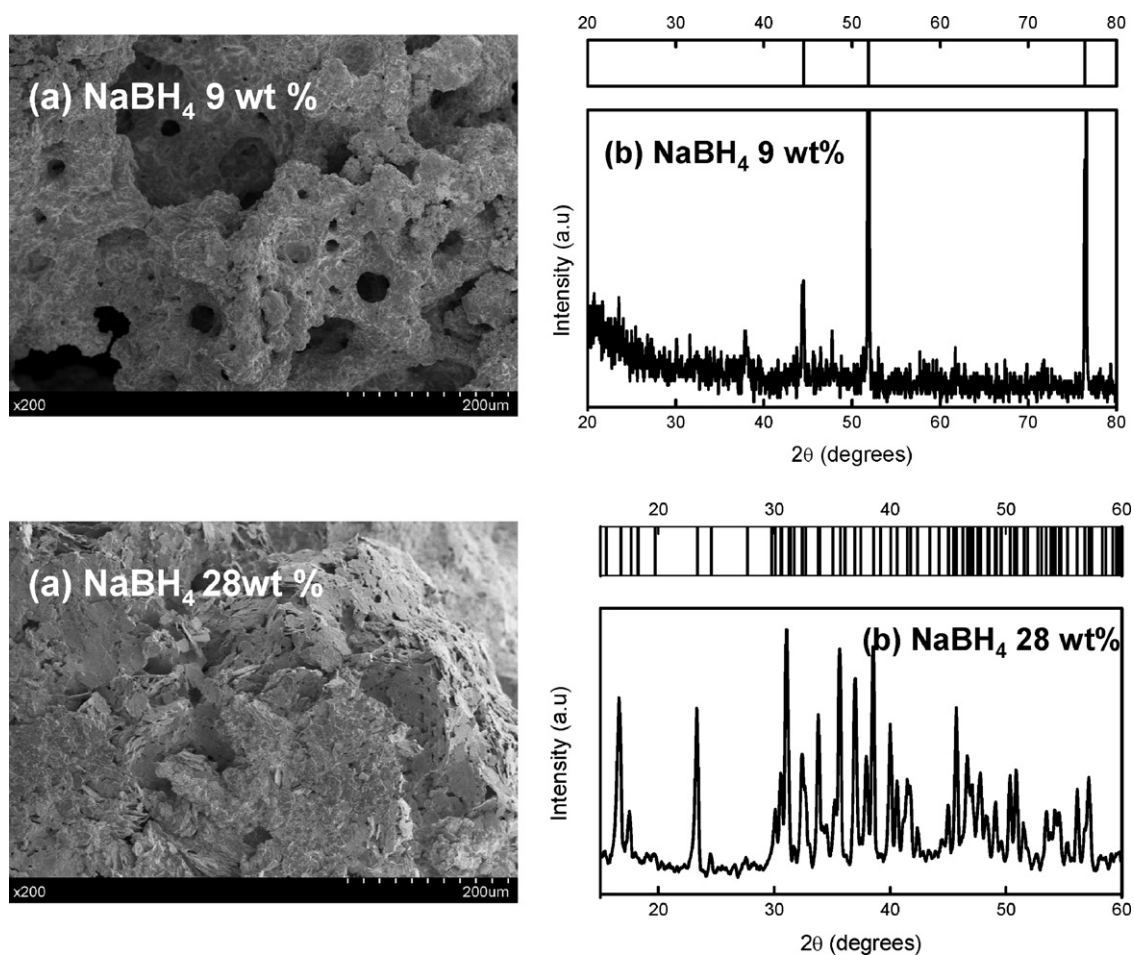
Fig. 5. (a) SEM images of the catalyst after reaction with 9 wt% and 28 wt% SBH fuel concentration. (b) XRD of the catalyst after reaction with 9 wt% (upper layer with XRD pattern of Ni[0]) and 28 wt% SBH fuel concentration (upper layer with XRD pattern of NaB(OH)$_4$).

Table 4
Parameters (as described in the text) for the third set of hydrogen generation kinetic measurements (exps. 3.a and 3.b) in comparison to the experiment 2.c.

Exp.	NaBH$_4$ concentration (wt%)	Fuel addition rate (ml min^{-1})	Mass of CoB (mg)	HGR (L min^{-1})	TC (%)	HSC (wt%)	HSC[a] potential (wt%)	T (°C)
3.a	19	0.52	388	0.25	82	3.3	4	41.5
3.b	19	1.2	680	0.6	86	3.4	4	54
2.c	19	2.5	675	1.16	90	3.5	4	60

[a] Considering that we are below the x_0 value for $X = 2$ in all cases.
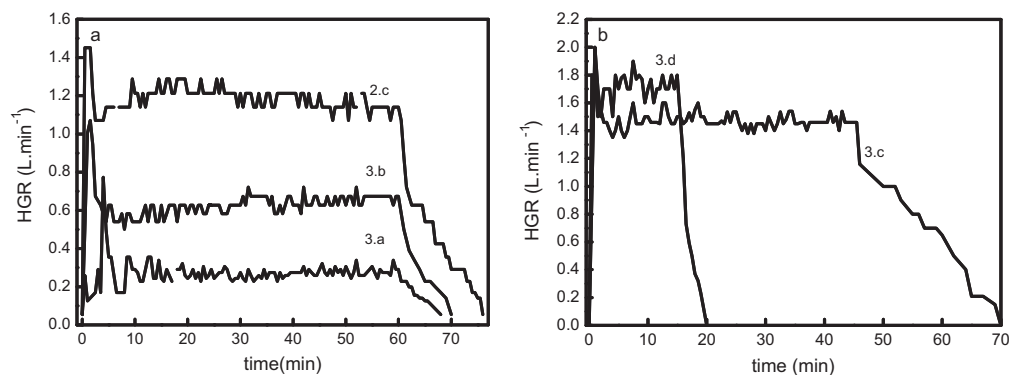

Fig. 6. Evolution of hydrogen generation rate for the third set of experiments (a) Experiments 3.a and 3.b in comparison to experiment 2.c. (b) Experiments 3.c and 3.d.
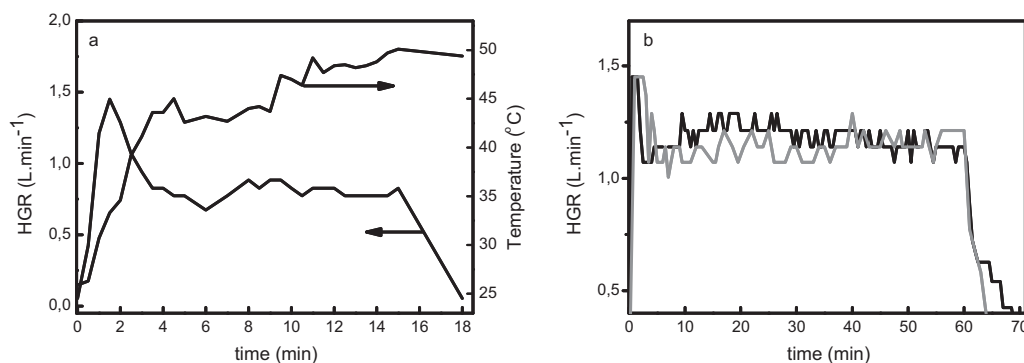
Fig. 7. (a) Evolution of hydrogen generation rate and temperature for a used supported catalyst after washing with water. (b) Evolution of hydrogen generation rate for a used supported catalyst after washing and reactivation (experiment rep. 2, grey curve) in comparison to the original experiment 2.c (black curve).

Table 5
Parameters (as described in the text) for the durability experiments (rep. 1–3) in comparison to the original experiment 2.c.

Exp.	NaBH$_4$ concentration (wt%)	Fuel addition rate (ml min^{-1})	HGR (L min^{-1})	TC (%)	HSC (wt%)	HSC[a] potential (wt%)	T (°C)
2.c	19	2.5	1.16	90	3.5	4	60
Rep. 1	19	2.1	1.0	90	3.5	4	58
Rep. 2	19	2.16	1.06	93	3.7	4	60
Rep. 3	19	1.93	0.97	95	3.8	4	56

[a] Considering that we are below the x_0 value for $X = 2$ in all cases.

1 L min^{-1}. Data are represented in Fig. 6(b) for a fuel addition rate (4 ml min^{-1}) calculated to produce 1.8 L min^{-1} hydrogen. Experiment 3.c was carried out with 785.5 mg of supported catalyst (far from the excess of catalyst regime). Under these conditions a HGR value of 1.45 L min^{-1} during around 45 min of fuel addition was measured. TC was around 65% and HSC was 2.6 wt%. To optimize these parameters a new experiment 3.d (see Fig. 6(b)) was done in excess of catalyst (1.34 g supported catalyst). The experiment was stopped after 15 min of fuel addition when fuel solution started to pass from the reactor to the washing flask. A higher volume reactor will be needed to work for longer periods at such high HGR values. A 1.7 L min^{-1} HGR was obtained for 15 min in optimized conditions.

3.3.4. Durability of the supported catalyst

Additional experiments were performed to test the possibility of reusing the catalyst. Two strategies were tested: (i) washing with MilliQ water the used supported catalyst in experiment 2.c after one month of open air storage and (ii) washing with MilliQ water and activating the supported catalyst used in (i) after five moths of open air storage (experiment rep. 1). The washing step is aimed to eliminate rests of hydrated borates deposited onto the catalyst. It has been proposed [21]) that aging of the catalyst in absence of SBH supply is due to the formation of Co(OH)$_2$ species according to Eq. (6).

$$Co_2B(s) + OH^-(ac) + 7H_2O(l) \rightarrow 2Co(OH)_2(s) + B(OH)_4^-$$
$$+ 3.5H_2(g) \quad (6)$$
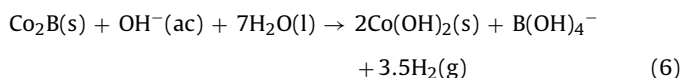
Reactivation of the catalyst [21] upon new addition of SBH occurs according to Eq. (7).

$$2Co(OH)_2(s) + BH_4^-(ac) \rightarrow Co_2B(s) + 0.5H_2(g) + OH^-(ac)$$
$$+ 3H_2O(l) \quad (7)$$
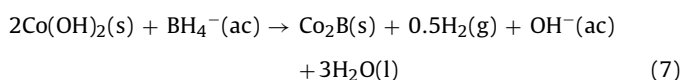
The activation step consisted of immersing the catalyst in a 9 wt% SBH in 4.5 wt% NaOH solution for 15 min. Repetitions of the washing/activation and catalytic test cycles were done twice on the supported catalyst used in (ii) (experiments rep. 2 and rep. 3). Results are summarized in Table 5. Fig. 7(a) shows the HG test

for case (i) while Fig. 7(b) shows case (ii) for experiment rep. 2 in comparison to the original data from experiment 2.c. All repetition experiments were done in the same conditions as experiment 2.c except for small variations in the fuel addition rate (see Table 5). It is clear from the figure that the activation step is a crucial point for a complete reproducibility of hydrogen evolution rate and therefore storage parameters. Reusing of the catalyst under these conditions has been demonstrated for at least 3 times without deterioration of performance. Loss of catalyst during the regeneration steps due to adhesion problems is the main hindrance to durability. It has been demonstrated here that ageing of the catalyst in open air conditions without washing for long periods (at least 6 months) is reversible through a reactivation step. In situ regeneration is not recommended due to bad quality of run-in periods (see Fig. 7(a)) and inadequate SBH concentration (19 wt% vs 9 wt%) and poor contact between catalyst and regeneration solution.

4. Conclusions

In the present paper a study is presented to optimize the catalyzed hydrolysis of SBH in a semi-continuous reactor to produce constant hydrogen flows of 1 L min^{-1}. Ni foam supported CoB catalyst was selected for this study.

A simple and low cost semi-continuous device is presented that operates at constant temperature by the controlled addition of SBH stabilized solutions without additional thermostatization.

Valuable theoretical considerations have been presented here to define the maximum achievable parameters in any optimized device. The effect of hydration of borate products and the solubility limits of reactants and products have been adequately considered and discussed.

It has been demonstrated that for each SBH concentration, the use of the adequate amount of catalyst and the feeding of the reactor with the necessary fuel rate to produce the desired 1 L min^{-1} hydrogen flow; maximizes the hydrolysis yield and therefore the hydrogen storage capacity. It was demonstrated that this model works well up to SBH concentrations of 19 wt%. For higher values it was difficult to stabilize the reactor temperature and borate precipitation also deteriorated the catalyst.

Optimized conditions were found for 19 wt% SBH solutions in 4.5 wt% NaOH, feeding the reactor at 2.5 ml min^{-1} to generate stable hydrogen flows of 1.16 L min^{-1} with a total fuel conversion of 90% and a gravimetric storage capacity (considering weight of fuel solution and catalysts) of 3.5 wt%. Run-in periods for stabilization of the hydrogen flow were found to be less than 5 min long. Experiments were also included for a wide range of HGR (0.2–1.7 L min^{-1}) with the same working hypothesis.

For optimized conditions it has been also shown that regeneration of the catalyst can be achieved by water washing and exposure to a SBH solution for 15 min. This procedure allows to reuse the catalyst for at least 3 cycles maintaining all the optimized parameters without significant changes.

In summary, an optimized semi-continuous reactor for the hydrolysis of SBH has been presented that could fulfil the requirements for a 60 W PEMFC for portable applications. Constant flow, constant temperature (below 100 °C), low run-in periods and maximization of TC and HSC have been pursued. Additionally, the system operates at room temperature without additional energy supply except for the peristaltic pump and the simplicity of the proposed set-up facilitates a reduction in the device volume.

Acknowledgements

References

[1] U.B. Demirci, O. Akdim, P. Miele, Int. J. Hydrogen Energy 34 (2009) 2638–2645.
[2] L. Schlapbach, A. Züttel, Nature 414 (2001) 353–358.
[3] J.C. Ingersoll, N. Mani, J.C. Thenmozhiyal, A. Muthaiah, J. Power Sources 173 (2007) 450–457.
[4] B.H. Liu, Z.P. Li, J. Power Sources 187 (2009) 527–534.
[5] U.B. Demirci, O. Akdim, J. Andrieux, J. Hannauer, R. Chamoun, P. Miele, Fuel Cells 3 (2010) 335–350.
[6] H.I. Schlesinger, H.C. Brown, A.E. Finholt, J.R. Gilbreath, H.R. Hoekstra, E.K. Hyde, J. Am. Chem. Soc. 75 (1953) 215–219.
[7] J.C. Walter, A. Zurawski, D. Montgomery, M. Thornburg, S. Revankar, J. Power Sources 179 (2008) 335–339.
[8] E.Y. Marrero-Alfonso, J.R. Gray, T.A. Davis, M.A. Matthews, Int. J. Hydrogen Energy 32 (2007) 4723–4730.
[9] C. Wu, F. Wu, Y. Bai, B. Yi, H. Zhang, Mater. Lett. 59 (2005) 1748–1751.
[10] J. Lee, K.Y. Kong, C.R. Jung, E. Cho, S.P. Yoon, J. Han, T.G. Lee, S.W. Nam, Catal. Today 120 (2007) 305–310.
[11] S.J. Kim, J. Lee, K.Y. Kong, C.R. Jung, I.G. Min, S.Y. Lee, H.J. Kim, S.W. Nam, T.H. Lim, J. Power Sources 170 (2007) 412–418.
[12] P.P. Prosini, P. Gilson, J. Power Sources 161 (2006) 290–293.
[13] D. Gervasio, S. Tasic, F. Zenhausern, J. Power Sources 149 (2005) 15–21.
[14] R. Oronzio, G. Monteleone, A. Pozio, M. De Francesco, S. Galli, Int. J. Hydrogen Energy 34 (2009) 4555–4560.
[15] Q. Zhang, G.M. Smith, Y. Wu, Int. J. Hydrogen Energy 32 (2007) 4731–4735.
[16] B.H. Liu, Z.P. Li, S. Suda, J. Alloys Compd. 468 (2009) 493–1493.
[17] A. Züttel, A. Borgschulte, S.-I. Orimo, Scripta Mater. 56 (2007) 823.
[18] F. Schüth, B. Bogdanovic, M. Felderhoff, Chem. Commun. (2004) 2249.
[19] D. Hua, Y. Hanxi, A. Xinping, C. Chuansin, Int. J. Hydrogen Energy 28 (2003) 1095–1100.
[20] Y. Kojima, Y. Kawai, H. Nakanishi, S. Matsumoto, J. Power Sources 135 (2004) 36–41.
[21] A. Garron, D. Świercyzński, S. Bennici, A. Auroux, Int. J. Hydrogen Energy 34 (2009) 1185–1199.